Eur. Phys. J. D **20**, 339–345 (2002)
DOI: 10.1140/epjd/e2002-00165-4

THE EUROPEAN PHYSICAL JOURNAL D

Isolation of adenine salts in the gas phase from a liquid beam of aqueous solutions by IR laser irradiation

J.-Y. Kohno, F. Mafuné, and T. Kondow[a]

East Tokyo laboratory, Genesis Research Institute, Inc. and Cluster Research Laboratory,
Toyota Technological Institute 717-86 Futamata, Ichikawa, Chiba 272-0001, Japan

Received 1st May 2002
Published online 13 September 2002 –

Abstract. A continuous liquid flow in a vacuum (a liquid beam) of an aqueous solution of adenine salt containing hydrochloric acid or sodium hydroxide was irradiated with an intense pulsed IR laser at 3 μm, which is resonant to a vibrational mode related to the OH stretch vibration of H_2O. Neutral species isolated into the vacuum were ionized by a pulsed UV laser at 270 nm, and the product ions were mass-analyzed by a time-of-flight mass spectrometer. It is found that $AH_2^{2+}\cdot 2Cl^-$ and $[A\text{–}iH]^{i-}\cdot iNa^+$ (i = 1–3) are isolated in the vacuum from the aqueous acidic and alkaline solutions, respectively, under irradiation of the IR laser, and undergo four-photon ionization involving decomposition and proton transfer of the intermediate species under irradiation of the UV laser.

PACS. 61.80.Ba Ultraviolet, visible, and infrared radiation effects (including laser radiation) – 68.03.-g Gas-liquid and vacuum-liquid interfaces – 82.39.Pj Nucleic acids, DNA and RNA bases

1 Introduction

Biological molecules function properly in an aqueous solution in cooperation with the solvent water molecules; any protein and DNA molecules could not function in aqueous solutions if the solvent water molecules do not interact with the protein and the DNA molecules. It is well-known that water molecules are actively involved in forming specific structures of protein and DNA molecules *in vivo*, in promoting the catalytic activity of enzymes, in helping proton transfer, and so forth. Such molecular functions in aqueous solutions can be elucidated through investigating the function of each component molecule and its ensemble with solvent water molecules, which are isolated in the gas phase. It should be noted that biological molecules function properly only in an aqueous salt solution but not in pure water in which they are denaturized and lost their innate functions. Accordingly, it is important to investigate the properties of these molecules isolated from aqueous salt solutions into the gas phase.

Various isolation techniques have been developed to this end. Nucleic acid bases gasified by heating or laser ablation are introduced into a supersonic molecular beam, and are subjected for spectroscopic measurements such as electronic spectroscopy [1–5], vibrational spectroscopy [6], photoelectron spectroscopy [7] and Rydberg electron attachment spectroscopy [8,9]. Their electronic and geometric structures have been elucidated. Fragmentation and reactions involving nucleic acid bases and their hydrated clusters have also been investigated [10,11]. Electrospray is a handy and versatile method, by which multiply charged molecules are readily introduced into a vacuum with a less extent of decomposition, but the multiple charges cause to modify and/or deform the intrinsic properties of the molecules more or less [12,13]. Matrix-assisted laser desorption/ionization (MALDI) is often employed to isolate biological molecules in a matrix; the molecules thus isolated are readily ionized by photoionization with laser irradiation [14–17]. In addition to these methods, molecular ions in a liquid beam are isolated in the gas phase by IR-laser desorption (laser induced-liquid beam ionization/desorption or LILBID) [18–23].

We have developed a method that molecules in a liquid beam are isolated from a liquid beam under irradiation of an IR laser having a wavelength resonant to a OH stretching vibration of liquid water [24–26]. In the present study, we applied this method to isolate adenine salts (probably adenine di-hydrochloride and sodium adeninate) from a liquid beam of aqueous acidic and alkaline solutions of adenine under irradiation of an IR laser (Scheme 1).

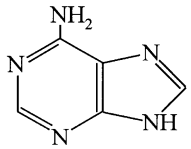

Scheme 1. Structural formula of adenine.

[a] e-mail: kondow@utsc.s.u-tokyo.ac.jp

The isolated adenine salts are ionized in the gas phase by a UV laser. We discussed the two different mechanisms of the isolation and the ionization of the adenine salts.

2 Experimental section

The apparatus employed in the experiment has been described in detail previously [24–26]. Hence, an overview of the apparatus, with details relevant to the present experiment is summarized. A continuous laminar liquid flow (liquid beam) of an aqueous solution was introduced into a vacuum chamber from a nozzle having an aperture with 20 μm in diameter. The sample solutions used were a 0.1-M adenine aqueous solution containing 0.2-M hydrochloric acid (0.1-M solution of adenine dihydrochloride (A·2HCl)) or that containing $(0.1 + \alpha)$-M sodium hydroxide (0.1-M solution of $[A–iH]^{i-}\cdot i Na^+$ $(i = 1–3)$), where α is less than 0.02. The continuous liquid flow was supplied by a Shimadzu LC-6A pump designed for a liquid chromatograph. The flow rate was maintained at 0.2 ml/min with a stagnation pressure of typically 20 atm inside the pump. The source chamber was evacuated by a 1 200 l s^{-1} diffusion pump and a liquid N_2 trap to attain a pressure down to 10^{-5}–10^{-6} torr during injection of the liquid beam. Commercially available adenine, hydrochloric acid, sodium hydroxide and water (deionized and distilled) were used without further purification. After traveling a distance of 2 mm from the nozzle, the liquid beam was crossed with an IR laser (3 μm) in the first acceleration region of the TOF mass spectrometer. The IR laser beam was generated by a Laser Vision IR–OPO system. In dealing with solutions of light and heavy water, the IR laser was tuned so as to excite the OH and OD stretching vibration mode of light or heavy water at 3 400 cm^{-1} (3 μm) and 2 630 cm^{-1} (3.8 μm), respectively. A UV laser beam (270 nm) was focussed 0.5 mm away from the liquid beam to ionize the ejected species at a delay time of $\sim$1 μs after the IR laser irradiation. The UV laser beam was obtained by frequency-doubling the output of a Quanta-ray PDL-3 dye laser pumped by the third harmonic of a Quanta-ray GCR-3 Nd:YAG laser. The pulse width of both the IR and the UV lasers is $\sim$8 ns. The laser power (typically $\sim$3 and $\sim$0.1 mJ/pulse for the IR and the UV lasers, respectively) was monitored by a LAS PM-200 energy meter. The IR and UV lasers were independently focused by lenses with the focal lengths of 450 and 500 mm, respectively. The fluence of the IR laser at the liquid beam was obtained from the diameter of a burning spot ($\sim 2.26 \times 10^{-3}$ cm^2) on a thermo-sensible paper.

The mass-to-charge ratios, m/z, of ions produced in the gas phase were analyzed by a reflectron TOF mass spectrometer. The ions were accelerated by a pulsed electric field in the direction perpendicular to both the liquid and the laser beams after a delay time of 1 μs after the photionization, and steered and focused by a set of vertical and horizontal deflectors and an einzel lens. Traveling in a 1.5-m field-free flight tube, the ions were reversed by a reflectron which provides a reversing field tilted by 2° off the beam axis. A train of spatially mass-selected ions were detected by a Daly detector after traveling another 0.5-m field-free region. Signals from the detector were amplified and processed by a LeCroy LT372 digital oscilloscope based on a microcomputer. The mass resolution, defined as $m/\Delta m$, was typically 70 at ordinary experimental conditions due to a wide energy distribution of the product ions.

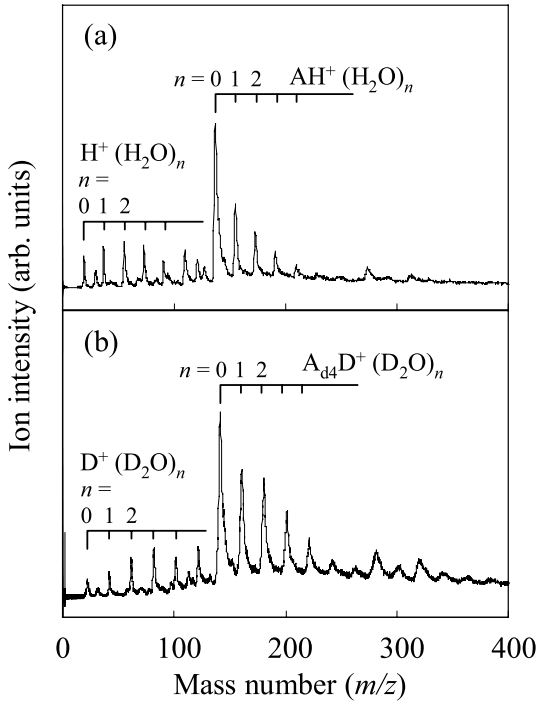

Fig. 1. Panel (a) shows a typical mass spectrum of ions produced from the liquid beam of a 0.1-M aqueous solution of A·2HCl under irradiation of an IR laser (3 μm) and a UV laser (270 nm) with a delay time of 2 μs. The IR laser is focused onto the liquid beam, whereas the UV laser is focused 0.5 mm away from the liquid beam. Peaks in the mass spectrum are assigned to a protonated adenine ion and its hydrated cluster ions, $AH^+(H_2O)_n$ $(n = 0–5)$ and protonated water clusters, $H^+(H_2O)_n$ $(n = 0–5)$. Panel (b) shows a typical mass spectrum of ions produced from the liquid beam of a solution of A·2DCl in D_2O under irradiation of an IR laser (3.8 μm) and a UV laser (270 nm) with a delay time of 2 μs. Peaks in the mass spectrum are assigned to $A_{d4}D^+(D_2O)_n$ $(n = 0–5)$ and $D^+(D_2O)_n$ $(n = 0–5)$ where A_{d4} represents 6,6,8,9-tetradeuterated adenine.

Multiphoton absorption spectra of product ions were obtained by scanning the wavelength of the UV laser. Intensities of different product ions were measured simultaneously for each 0.0024 nm step.

3 Results

Figure 1a shows a mass spectrum of ions produced from a 0.1-M aqueous solution of A·2HCl under irradiation of an IR laser (3 μm) with subsequent irradiation of a UV laser (270 nm) at 2 μs after the IR laser firing. The IR laser was focused onto a liquid beam, whereas the UV laser

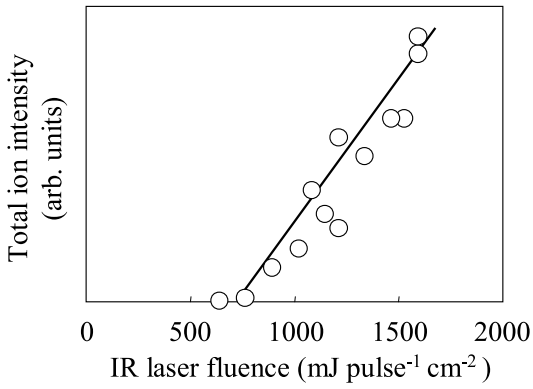

Fig. 2. Total intensity of ions produced from an aqueous solution of A·2HCl as a function of the fluence of the incident IR laser. The power of the UV laser is set to 40 μJ pulse^{-1}. The ions start to appear at a threshold fluence ($\sim$800 mJ pulse^{-1} cm^{-2}) and increase with increase in the laser fluence.

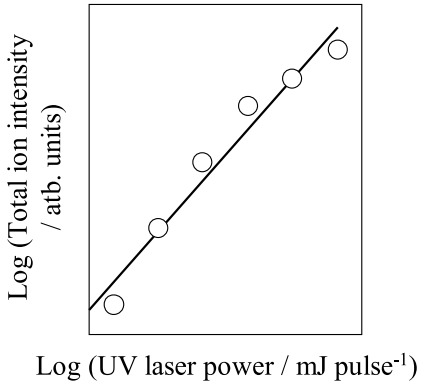

Fig. 3. Logarithmic plots of the total intensity of ions, AH^+ $(H_2O)_n$ (n = 0–5), produced from an aqueous solution of A·2HCl against the power of the incident UV laser. The fluence of the IR laser is set to 1 600 mJ pulse^{-1} cm^{-2}. A solid line represents the fitting result by equation (1) (see text).

was focused 0.5 mm away from the liquid beam. Peaks in the mass spectrum are assigned to a protonated adenine ion, its hydrated cluster ions, AH^+ $(H_2O)_n$ (n = 0–5) and protonated water clusters, H^+ $(H_2O)_n$ (n = 0–5). In order to confirm the mass assignment mentioned above, heavy water (D_2O) is used instead of H_2O as a solvent. Figure 1b shows a typical mass spectrum of ions produced from a solution of A·2DCl in D_2O by irradiation of an IR laser (3.8 μm) and a UV laser (270 nm) with a delay time of 2 μs. Peaks in the mass spectrum are assigned to $A_{d4}D^+$ $(D_2O)_n$ (n = 0–5) and D^+ $(D_2O)_n$ (n = 0–5) where A_{d4} represents 6,6,8,9-tetradeuterated adenine. The observation of $A_{d4}D^+$ $(D_2O)_n$ (n = 0–5) and D^+ $(D_2O)_n$ (n = 0–5) support the present mass assignment on the basis of the fact that the 6,6,8,9 positions of adenine are known to be fully deuterated in a D_2O solution [27].

Figure 2 shows the total intensity of the ions produced from an acidic aqueous solution of adenine as a function of the fluence of the incident IR laser. The power of the UV laser was set to be 40 μJ pulse^{-1}. The ions start to

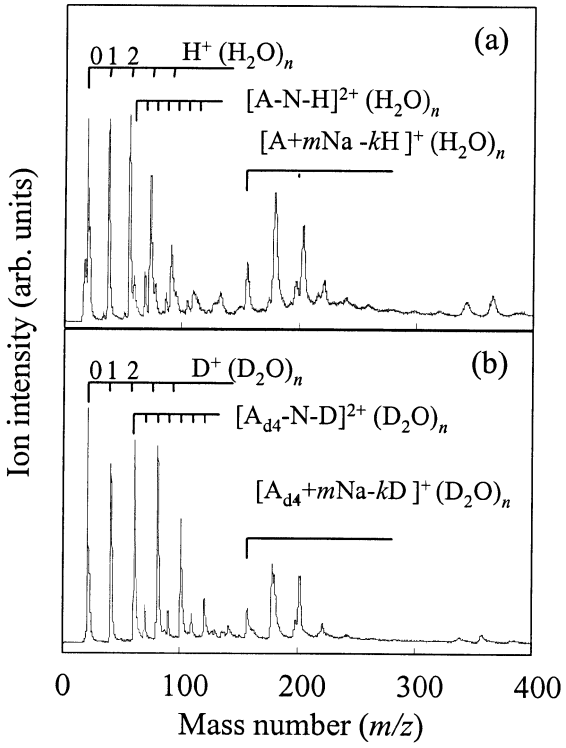

Fig. 4. Mass spectra of ions produced from a liquid beam of a 0.1-M adenine containing $(0.1+\alpha)$-M sodium hydroxide in (a) H_2O and (b) D_2O by irradiation of an IR laser (3 and 3.8 μm for panels (a) and (b), respectively) and a UV laser (270 nm) with a delay time of 2 μs. The isotope shift demonstrated in these mass spectra lead us to conclude that H^+ $(H_2O)_n$ (n = 0–5) and $[A+mNa-kH]^+$ $(H_2O)_n$ are produced. In addition to the ions, doubly charged ions, $[A–N–H]^{2+}$ $(H_2O)_n$, are found to be produced.

appear at the threshold fluence ($\sim$800 mJ pulse^{-1} cm^{-2}) and increase with increase in the laser fluence.

Figure 3 shows logarithmic plots of the total intensity, T, of the ions, AH^+ $(H_2O)_n$ (n = 0–5), produced from an aqueous acidic solution of adenine against the power of the incident UV laser, I_{UV}. The fluence of the IR laser was set to be 1 600 mJ pulse^{-1} cm^{-2}. The dependence of the total intensity on the power of the UV laser is expressed in terms of the formula,

$$T = C\, {I_{UV}}^a, \tag{1}$$

where a represents the number of photons involved in the ionization and C is a constant. The value of a is obtained to be 3.9 ± 0.13 from the slope of the T *vs.* I_{UV} plots; the ions are produced by absorbing four photons during the ionization. Similarly, four photons were found to be involved for the production of every product ion.

Figure 4a shows a typical mass spectrum of ions produced from a liquid beam of a 0.1-M adenine containing $(0.1+\alpha)$-M sodium hydroxide in H_2O by irradiation of an IR laser (3 μm) and a UV laser (270 nm) with a delay time of 2 μs. Figure 4b shows a typical mass spectrum of ions produced from the corresponding deuterated solution under irradiation of the IR laser at 3.8 μm. The comparison

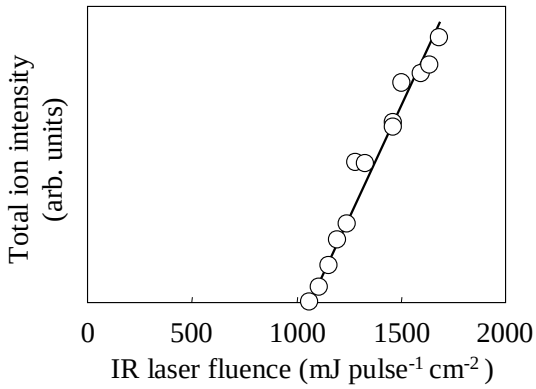

Fig. 5. Total intensity of ions produced from a solution of 0.1-M adenine containing $(0.1+\alpha)$-M sodium hydroxide in D_2O as a function of the fluence of the incident IR laser. The power of the UV laser is set to 90 μJ pulse^{-1}. The ions start to appear at a threshold fluence ($\sim$1 000 mJ pulse^{-1} cm^{-2}) and increase with increase in the laser fluence.

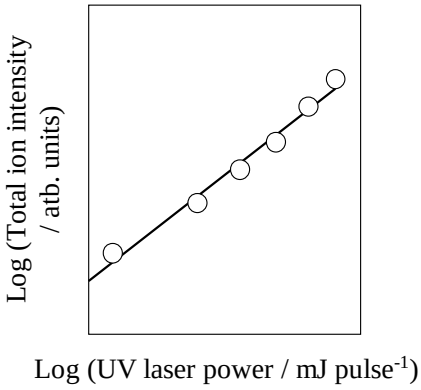

Fig. 6. Logarithmic plots of total intensity of ions produced from a solution of 0.1-M adenine and $(0.1+\alpha)$-M sodium hydroxide in D_2O against the power of the incident UV laser. The fluence of the IR laser is set to 1 500 mJ pulse^{-1} cm^{-2}. A solid line represents the fitting result by equation (1) (see text).

of these two spectra lead us to conclude that H^+ $(H_2O)_n$ ($n = 0$–5) and $[A+m\mathrm{Na}-k\mathrm{H}]^+$ $(H_2O)_n$ ($(m, k) = (1, 2)$, (2, 2), (2, 3) and (3, 3)) are produced. In addition, doubly charged ions, $[\mathrm{A–N–H}]^{2+}$ $(H_2O)_n$, are also produced. Note that the inside of the parentheses, [ ], represents the molecular formula of the ion and the subsequent superscript of that does the charge of the ion.

Figure 5 shows the total intensity of the ions produced from a solution of 0.1-M adenine containing $(0.1+\alpha)$-M sodium hydroxide in D_2O as a function of the fluence of the incident IR laser. The power of the UV laser was set to be 90 μJ pulse^{-1}. The ions start to appear at the threshold fluence ($\sim$1 000 mJ pulse^{-1} cm^{-2}) and increase with increase in the laser fluence.

Figure 6 shows logarithmic plots of the total intensity of the ions produced from a solution of 0.1-M adenine and $(0.1+\alpha)$-M sodium hydroxide in D_2O against the power of the incident UV laser. The fluence of the IR laser was set to be 1 500 mJ pulse^{-1} cm^{-2}. The dependence of the intensity on the UV-laser power is fit by using equation (1), giving the value of a to be 4.5 ± 0.09; the ions are produced by absorbing about four photons during the ionization. All the ions observed are found to be produced by absorbing about four photons.

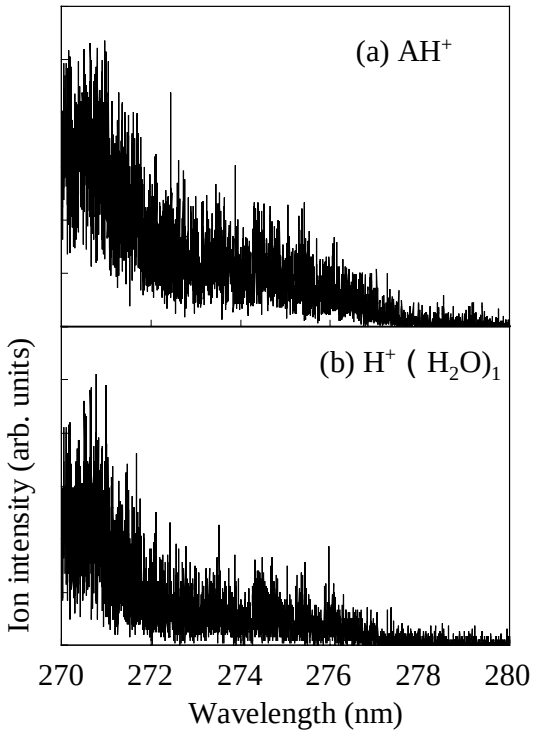

Fig. 7. Ion intensities of (a) AH^+ and (b) H^+ $(H_2O)_1$ as a function of the UV-laser wavelength (multiphoton absorption spectra). Each multiphoton absorption spectrum exhibits one broad structure.

Figure 7 shows the ion intensities of AH^+ and H^+ $(H_2O)_1$ in panels (a) and (b), respectively, as a function of the UV-laser wavelength (multiphoton absorption spectra). One broad band is observed in each multiphoton absorption spectrum. However, no significant variation of the ion intensity with the laser wavelength was observed when the alkaline solution was used.

The intensities of all the ions observed were measured at different concentrations of A·2HCl as follows: An aqueous acidic solution of adenine (or an aqueous solution of A·2HCl) in a sample reservoir was changed to pure water at a given time. The concentration of A·2HCl in the liquid beam decreases gradually with time. It takes several tens of minutes to be changed with pure water in the liquid beam, because the reservoir is connected to the liquid beam nozzle by a thin and long tube. The ion intensities were measured as a function of the time after the reservoir was changed to pure water. The dependence of the ion intensities on the elapsed time is equivalent to the dependence of the ion intensities on the concentration of A·2HCl. Figure 8 shows the intensities of AH^+ and H^+ $(H_2O)_1$ as a function of the elapsed time after the change of an aqueous solution of A·2HCl to pure water in the sample reservoir. The time dependence of the H^+

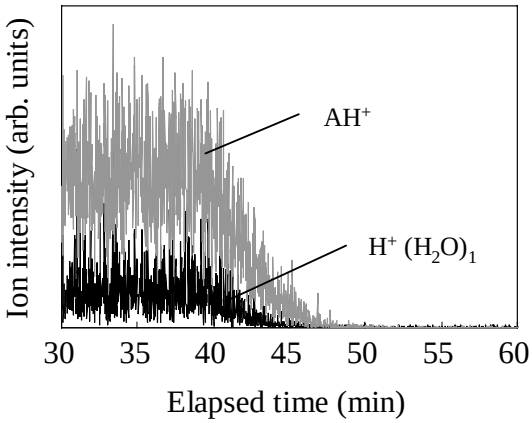

Fig. 8. Intensities of AH^+ and H^+ $(H_2O)_1$ as a function of the elapsed time from the change of an aqueous solution of A·2HCl to pure water in the sample reservoir. The time dependence of the H^+ $(H_2O)_1$ intensity agrees with that of the AH^+ intensity; in both cases, the intensity starts to decreases at about 40 minutes and vanishes at about 50 minutes after the change of the reservoir content.

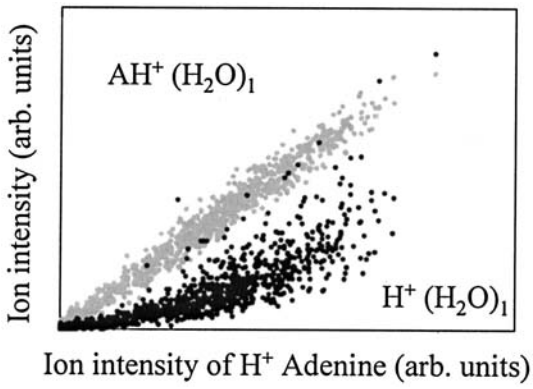

Fig. 9. Intensities of AH^+ $(H_2O)_1$ and H^+ $(H_2O)_1$ as a function of the intensity of AH^+ measured simultaneously.

$(H_2O)_1$ intensity agrees with that of the AH^+ intensity; in both cases, the intensity starts to decreases at about 40 minutes and vanishes at about 50 minutes after the change of the reservoir content. The intensity decrease occurring at almost the same elapsed time implies that the protonated water clusters are produced *via* the laser excitation of A·2HCl. Figure 9 shows the intensities of AH^+ $(H_2O)_1$ and H^+ $(H_2O)_1$ as a function of the intensity of AH^+ measured simultaneously. The obtained relationship of I_{X^+} (the intensity of an ion, X^+) *vs.* I_{AH^+} are analyzed by the following relation,

$$I_{X^+} = B{I_{AH^+}}^b, \tag{2}$$

where b represents the number of A·2HCl for the production of X^+ on the assumption that one A·2HCl is involved for the production of AH^+, and B is constant. The values of b are obtained to be 1.03 and 1.37 for AH^+ $(H_2O)_1$ and H^+ $(H_2O)_1$, respectively.

4 Discussion

4.1 Ejection of adenine salts in the gas phase

As shown in Figure 1, protonated adenine clusters, AH^+ $(H_2O)_n$, and protonated water clusters, H^+ $(H_2O)_n$, are produced under irradiation of an IR laser (3 μm) onto the liquid beam of a 0.1-M aqueous solution of A·2HCl and subsequent photoionization at a distance of 0.5 mm away from the liquid beam by a UV laser (270 nm) with a delay time of $\sim$1 μs after the IR laser firing. Irradiating the liquid beam with the IR or the UV laser alone formed no ion. These findings indicate that neutral species are isolated in the gas phase by the IR laser irradiation and are photoionized by the UV laser. Adenine salts, A·2HCl and $[A\text{–}iH]^{i-}\cdot i Na^+$, (see Sects. 4.2 and 4.3) are ejected into the gas phase from the liquid beam of aqueous acidic and alkaline solutions of adenine, respectively, by the IR laser irradiation. Ejection of the neutral species requires at least a laser fluence of 800 $\sim$ 1 000 mJ pulse^{-1} cm^{-2}, above which the abundance of the species increase with increase in the laser fluence (see Figs. 2 and 4). The adenine salts can only be released from the liquid beam surface if a photon energy introduced in the solution supersedes the solvation energy of the salts. Therefore, the salts start to be isolated above the threshold fluence.

4.2 Formation of ion from an aqueous acidic solution

As an adenine molecule has basic nitrogen atoms, the molecule is dissolved in a HCl solution as a protonated form. The adenine molecule forms a salt, $AH_2^{2+}\cdot 2Cl^-$, in an aqueous solution of 0.1-M adenine and 0.2-M HCl. In fact, 0.1-M adenine is insoluble either in pure water or in an aqueous solution of less than 0.2-M HCl. The neutral species produced by the IR laser irradiation is assigned to be $AH_2^{2+}\cdot 2Cl^-$, because (1) the ionic components, AH_2^{2+} and $2Cl^-$, are actually present in the HCl solution, (2) hydrochloric acid is needed to dissolve adenine into water, and (3) the species is neutral. However, the species are not adenine molecules, because adenine molecules are dissolved in an aqueous solution of hydrochloric acid but not in pure water and the multiphoton absorption spectrum of the neutral species (see Fig. 7) is not explained simply by a broadening of that of adenine molecules [5]. Photionization of the neutral species, $AH_2^{2+}\cdot 2Cl^-$, by the UV laser gives AH^+, H^+, and their hydrated clusters.

The ion, AH^+, is produced by a four-photon ionization of $AH_2^{2+}\cdot 2Cl^-$ in the gas phase. As shown in Figure 7, the multiphoton absorption spectrum of $AH_2^{2+}\cdot 2Cl^-$ exhibits one significantly broad structure with the intensity maximum in the vicinity of $\sim$271 nm in wavelength. This spectrum is contrasted to the multi-peaked multiphoton absorption spectrum of adenine molecules in the gas phase measured by Kim and his coworkers in the corresponding wavelength region [5]. The broad structure is attributable to a short life time of the excited state of the adenine salt, $[AH_2^{2+}\cdot 2Cl^-]^{\ddagger}$, produced by absorbing

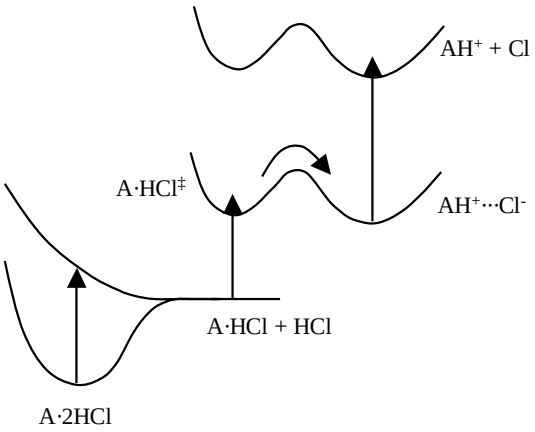

Scheme 2. Photoionization of A·2HCl.

the first photon; $AH_2^{2+}\cdot 2Cl^-$ in the excited state is fragmented promptly before absorbing the second photon. The following reaction scheme is conceivable under these circumstances: the neutral species, $AH_2^{2+}\cdot 2Cl^-$ is exited by absorbing the first photon and is promptly dissociated into $[AH^+\cdot Cl^-] + HCl$. This dissociation fulfils the energetics that the dissociation energy of $AH_2^{2+}\cdot 2Cl^-$ into $[AH^+\cdot Cl^-]$ and HCl (<1.4 eV [28]) is much less than the photon energy (4.6 eV) of the incident UV laser. The intermediate species, $[AH^+\cdot Cl^-]$, is excited into an ion pair state, $[AH^+\cdots Cl^-]$, by absorbing the second photon. Actually, Kim and his coworkers have reported similar ion pair formation in an excited state of a hydrated adenine [10]. We suggest that the following ionization process takes place after the isolation of $AH_2^{2+}\cdot 2Cl^-$ from the liquid beam (Scheme 2)

$$AH_2^{2+}\cdot 2Cl^- + h\nu \rightarrow [AH^+\cdot Cl^-] + HCl, \quad (3)$$

$$[AH^+\cdot Cl^-] + h\nu \rightarrow [AH^+\cdots Cl^-], \quad (4)$$

$$[AH^+\cdots Cl^-] + 2h\nu \rightarrow AH^+ + Cl + e^-. \quad (5)$$

The hydrated cluster ion, $AH^+ (H_2O)_1$, is produced by association of H_2O with AH^+ thus produced *via* the above processes; the $AH^+ (H_2O)_1$ intensity increases proportionally with increase in the AH^+ intensity (see Fig. 9). In contrast, $H^+ (H_2O)_n$ is produced mainly by collisional proton transfer from AH^+ to $(H_2O)_{n'}$

$$AH^+ + (H_2O)_{n'} \rightarrow A + H^+(H_2O)_n + (n'-n)H_2O, \quad (6)$$

because the $H^+ (H_2O)_n$ intensity is nearly proportional to the AH^+ intensity; in reality, the $H^+ (H_2O)_n$ intensity is found to be proportional to the AH^+ intensity to the power of 1.37. The deviation from the linearity is ascribable to the operation of an additional process to the production of $H^+ (H_2O)_n$ where one more $AH_2^{2+}\cdot 2Cl^-$ is involved in generating $H^+ (H_2O)_n$. The most likely process is

$$AH^+ + AH_2^{2+}\cdot 2Cl^- \rightarrow [A_2H_3^{3+}\cdot 2Cl^-], \quad (7)$$

$$[A_2H_3^{3+}\cdot 2Cl^-] + (H_2O)_{n'} \rightarrow [A_2H_2^{2+}\cdot 2Cl^-] + H^+(H_2O)_n + (n'-n)H_2O. \quad (8)$$

4.3 Formation of ion from an aqueous alkaline solution

In an aqueous alkaline solution of adenine, adenine is present in a form of $[A–H]^-$ at pKa of 4.07, $[A–2H]^{2-}$ at pKa of 9.67 and could be $[A–3H]^{3-}$ at a higher value of pKa. It is obvious, as argued in Section 4.2, that all the species, $[A–iH]^{i-}\cdot i Na^+$ (i = 1–3), present in the solution containing 0.1 M of NaOH should be isolated by the IR laser irradiation. These neutral species thus isolated are photoionized by the UV laser into $H^+ (H_2O)_n$ (n = 0–5) and singly charged ions, $[A + mNa - kH]^+ (H_2O)_n$ ((m, k) = (1, 2), (2, 2), (2, 3) and (3, 3)) (see Fig. 4) probably through three intermediate species, $[[A–iH]^{i-}\cdot i Na^+]^{2+}$ (i = 1–3). The involvement of these three intermediate species in the ionization is postulated because (1) doubly charged ions, $[A–N–H]^{2+} (H_2O)_n$, are produced in the photoionization (see Fig. 4) [29], and (2) the reaction intermediates postulated are produced directly by abstraction of two electrons from the species isolated from the liquid beam by the IR laser irradiation. The photoionization processes involving $[A–H]^-Na^+$ are expressed as follows:

$$[A–H]^-\cdot Na^+ + nh\nu \rightarrow [A–H]\cdot Na^+ \quad (9)$$

$$[A–H]\cdot Na^+ + n'h\nu \rightarrow [A–H]^+\cdot Na^+ \quad (10)$$

$$[A–H]^+\cdot Na^+ \rightarrow [A-N-H]^{2+} + NaN \quad \text{(decomposition)} \quad (11)$$

$$[A–H]^+\cdot Na^+ + (H_2O)_n \rightarrow [A–2H]\cdot Na^+ + H^+(H_2O)_n \quad \text{(proton transfer)}. \quad (12)$$

Similarly, the photoionization of $[A–2H]^{2-}\cdot 2Na^+$ are given as

$$[A–2H]^{2-}\cdot 2Na^+ + nh\nu \rightarrow [A–2H]\cdot 2Na^+ + 2e^- \quad (13)$$

$$[A–2H]\cdot 2Na^+ + (H_2O)_n \rightarrow [A–3H]^-\cdot 2Na^+ + H^+(H_2O)_n \quad \text{(proton transfer)} \quad (14)$$

$$[A–2H]\cdot 2Na^+ + (H_2O)_n \rightarrow [A–2H]^-\cdot 2Na^+ + (H_2O)_n^+, \quad \text{(charge transfer)} \quad (15)$$

where $(H_2O)_n^+$, should be decomposed immediately into $H^+ (H_2O)_{n'}$ in process (15). It is straightforward to conclude that $[A–3H]^{3-}\cdot 3Na^+$ is photoionized as

$$[A–3H]^{3-}\cdot 3Na^+ + nh\nu \rightarrow [A–3H]^-\cdot 3Na^+ + 2e^- \quad (16)$$

$$[A–3H]^-\cdot 3Na^+ + (H_2O)_n \rightarrow [A–3H]^{2-}\cdot 3Na^+ + (H_2O)_n^+ \quad \text{(charge transfer)}. \quad (17)$$

5 Conclusion

A liquid beam of an aqueous acidic or alkaline solution of adenine was irradiated with IR and UV lasers, and the product ions were mass-analyzed by a time-of-flight mass spectrometer. It is found that in the acidic solution, $AH_2^{2+}{\cdot}2Cl^-$ is ejected by the IR laser irradiation while $[A–iH]^{i-}{\cdot}iNa^+$ ($i = 1$–3) from the alkaline solution. The ionization mechanisms elucidated in the present study facilitates isolation of biologically important molecules into the gas phase from a buffer solution in which these molecules are dissolved.

The authors are grateful to Mr. Yoshihiro Takeda for his assistance in the early stage of the liquid beam. This research was supported by the Special Cluster Research Project of Genesis Research Institute, Inc.

References

1. Y. Tsuchiya, T. Tamura, M. Fujii, M. Ito, J. Phys. Chem. **92**, 1760 (1988)
2. B.B. Brady, L.A. Peteanu, D.H. Levy, Chem. Phys. Lett. **147**, 538 (1988)
3. E. Nir, L. Grace, B. Brauer, M.S. de Vries, J. Am. Chem. Soc. **121**, 4896 (1999)
4. E. Nir, Ch. Janzen, P. Imhof, K. Kleinermanns, M.S. de Vries, J. Chem. Phys. **115**, 4604 (2001)
5. N.J. Kim, G. Jeong, Y.S. Kim, J. Sung, S.K. Kim, Y.D. Park, J. Chem. Phys. **113**, 10051 (2000)
6. M.R. Viant, R.S. Fellers, R.P. McLaughlin, R.J. Saykally, J. Chem. Phys. **103**, 9502 (1995)
7. J.H. Hendricks, S.A. Lyapustina, H.L. de Clercq, K.H. Bowen, J. Chem. Phys. **108**, 8 (1998)
8. C. Desfrançois, H. Abdoul-Carime, S. Charles, V. Périquet, J.P. Schermann, D.M.A. Smith, L. Adamowicz, J. Chem. Phys. **110**, 11876 (1999)
9. C. Desfrançois, V. Périquet, Y. Bouteiller, J.P. Schermann, J. Phys. Chem. A **102**, 1274 (1998)
10. N.J. Kim, H. Kang, G. Jeong, Y.S. Kim, K.T. Lee, S.K. Kim, J. Phys. Chem. A **104**, 6552 (2000)
11. N.J. Kim, H. Kang, G. Jeong, Y.S. Kim, K.T. Lee, S.K. Kim, J. Chem. Phys. **115**, 7002 (2001)
12. R.R. Hudgins, M.F. Jarrold, J. Am. Chem. Soc. **121**, 3494 (1999)
13. M.F. Jarrold, Acc. Chem. Res. **32**, 360 (1999)
14. B.A. Budnik, K.B. Jensen, T.J.D. Jørgensen, A. Hasse, R.A. Zubarev, Rapid Commun. Mass. Spectrom. **14**, 578 (2000)
15. M. Amft, F. Moritz, C. Weickhardt, J. Grotemeyer, Int. J. Mass Spectrom. **167/168**, 661 (1997)
16. T. Wyttenbach, J.J. Batka Jr, J. Gidden, M.T. Bowers, Int. J. Mass Spectrom. **193**, 143 (1999)
17. T. Wyttenbach, M. Witt, M.T. Bowers, Int. J. Mass Spectrom. **182/183**, 243 (1999)
18. W. Kleinfort, J. Avdiev, B. Brutschy, Int. J. Mass Spectrom. **152**, 135 (1996)
19. W. Kleinfort, M. Schweitzerm, J.W. Engels, B. Brutschy, Int. J. Mass Spectrom. **156**, 195 (1996)
20. W. Kleinfort, M. Schweitzerm, J.W. Engels, B. Brutschy, Int. J. Mass Spectrom. **163**, 1 (1997)
21. F. Sobott, W. Kleinfort, B. Brutschy, Anal. Chem. **69**, 3587 (1997)
22. F. Sobott, A. Wattenberg, H. Barth, B. Brutschy, Int. J. Mass Spectrom. **185**, 271 (1999)
23. A. Wattenberg, F. Sobott, H. Barth, B. Brutschy, Int. J. Mass Spectrom. **203**, 49 (2000)
24. N. Horimoto, J. Kohno, F. Mafun, T. Kondow, J. Phys. Chem. A **103**, 9569 (1999)
25. N. Horimoto, J. Kohno, F. Mafun, T. Kondow, Chem. Phys. Lett. **318**, 536 (2000)
26. J. Kohno, F. Mafun, T. Kondow, J. Phys. Chem. A **105**, 8939 (2001)
27. K. Wüthrich, *NMR of Proteins and Nucleic Acids* (John Wiley & Sons, New York, 1986)
28. The dissociation energy of $AH_2^{2+}{\cdot}2Cl^-$ into $AH^+{\cdot}Cl^-$ and HCl is estimated as follows: at first, we assume that the dissociation energy of $AH_2^{2+}{\cdot}2Cl^-$ into $AH^+{\cdot}Cl^-$ and HCl, ΔE, is equal to that of $AH^+{\cdot}Cl^-$ into A and HCl. Following equations are obtained by thermodynamic considerations:

$$A(g) + HCl(g) = AH^+{\cdot}Cl^-(g) + \Delta E \quad \text{(a)}$$

$$A(g) = A(s) + a(33.5\ \text{kJ mol}^{-1}) \quad \text{(b)}$$

$$HCl(g) = HCl(s) + b(74.85\ \text{kJ mol}^{-1}) \quad \text{(c)}$$

$$AH^+{\cdot}Cl^-(g) = AH^+{\cdot}Cl^-(s) + c \quad \text{(d)}$$

$$A(s) + HCl(s) = AH^+{\cdot}Cl^-(s) + d(\sim 30\ \text{kJ mol}^{-1}). \quad \text{(e)}$$

The values of a and b are given in literatures. Secondly, we assume that the value of d is almost the same as the reaction energy of HCl and a weak alkaline molecule in an aqueous solution, which is given in literatures. The upper limit of the dissociation energy is then given as

$$\Delta E = (a + b - c + d) < (a + b + d) \sim 140\ \text{kJ mol}^{-1}\ (\sim 1.4\ \text{eV}).$$

29. The most probable assignment of the peak is $[A–N–H]^{2+}(H_2O)_n$, but we cannot exclude the formation of $[A–N–2H]^{2+}(H_2O)_n$ or $[A–N]^{2+}(H_2O)_n$ because the mass resolution is not high enough to resolve them